Backstepping cooperative control study of a 5-DOF magnetic levitation actuator for laser cutting lens control

Qinwei ZHANG*, Feng LIU**, Chuan ZHAO*, Feng SUN*, Xu BAI*, Honglei SHA**
*School of Mechanical Engineering, Shenyang University of Technology
No. 111, Shenliao West Road, Shenyang Economic and Technological Development Zone, Shenyang 110870, China
E-mail: zhaochuan@sut.edu.cn
**Tianjin EMAGING Technology Co.,Ltd.
No. 3, Xiaqing Road, West Zone, Tianjin Economic-Technological Development Area, Tianjin 300462, China
E-mail: lf13898984195@outlook.com

Abstract
During laser processing, optimizing the cutting effect by adjusting the angle or the off-axis displacement between the auxiliary gas and the laser beam has become an important approach to improving processing quality and efficiency. However, traditional electromechanical actuators have notable limitations in terms of compactness and multi-degree-of-freedom cooperative control, making them inadequate for the demands of high-speed and high-precision laser cutting. To address this issue, this paper designs a five-degree-of-freedom magnetic levitation actuator for controlling the laser cutting lens, and proposes a multi-degree-of-freedom cooperative control strategy based on backstepping control to handle the system's strong coupling, nonlinearity, and model uncertainty. First, a dynamic model of the drive system is established, and a backstepping controller is developed accordingly. Then, a centralized control strategy is formulated, and simulation and experimental comparisons are conducted between PID and backstepping control. The experimental results demonstrate that the proposed backstepping controller outperforms the traditional PID controller in terms of multi-degree-of-freedom cooperative control and dynamic response, effectively enhancing the system's multi-degree-of-freedom control performance. This study provides theoretical support and engineering guidance for designing control strategies in high-performance magnetic levitation drive systems.

Keywords : Laser cutting, Magnetic levitation actuator, PID, Backstepping control, Dynamic performance

1. Introduction

With increasing demands for geometric accuracy, surface quality, and micron-level dimensional control in manufacturing, laser cutting technology has been widely adopted in industrial applications due to its non-contact nature, high precision, and efficiency (Seyedeh et al., 2024). However, existing laser cutting systems still face limitations in processing complex curved surfaces or shaped workpieces, primarily due to the structural complexity and limited degrees of freedom of traditional contact-based drive mechanisms. These constraints hinder the realization of efficient and precise control of the cutting spot across arbitrary orientations.

Magnetic levitation actuators offer significant potential for multi-degree-of-freedom precision motion control owing to their frictionless operation, absence of mechanical wear, and rapid dynamic response (Liu et al., 2023). Compared to conventional contact-based actuators, they feature a compact structure and superior dynamic performance, making them highly promising for high-precision applications such as laser cutting lens control (Zhao et al., 2024). Nevertheless, the multi-degree-of-freedom control of magnetic levitation systems remains challenging due to inherent strong coupling, nonlinearity, and parameter uncertainty. While traditional PID control methods are commonly employed because of their simplicity, they often lack robustness against external disturbances and model uncertainties (Chen et al., 2017). To overcome these limitations, various advanced control strategies have been explored, including self-resilient control (Zhang et al., 2025), sliding mode control (Vimala et al., 2019), Lyapunov-based adaptive control (Zhang et al., 2018), fuzzy control (Li et al., 2022), and even deep learning-based approaches (Yao et al., 2019). Although these methods enhance system performance to varying degrees, they typically require accurate modeling and involve complex controller design processes, which can compromise the balance between practical implementation and robustness. Backstepping

control, as a recursive nonlinear control design method, offers a modular framework with a clear design logic grounded in Lyapunov stability theory (R.-J. et al., 2008). In recent years, it has shown promising results in applications such as spacecraft attitude control (Hu et al., 2022) and vibration suppression in magnetic bearings (Xu et al., 2024). However, its optimization for dynamic performance and practical application in multi-degree-of-freedom magnetic levitation actuators remains underexplored.

To address these gaps, this paper proposes a backstepping control strategy tailored for multi-degree-of-freedom magnetic levitation actuators used in laser cutting lens systems. A dynamic model of the actuator is first established, followed by the design of a backstepping controller. Simulation and experimental comparisons with conventional PID control are conducted to validate the effectiveness of the proposed method in improving multi-degree-of-freedom motion control performance.

2. System description

2.1 System structure and working principle

The structure of the five-degree-of-freedom magnetic levitation actuator is illustrated in Fig. 1. The system comprises a levitation platform, axial and radial electromagnets, and an aluminum frame. To achieve a compact design, the axial and radial electromagnets are arranged in a 45° cross configuration.

The working principle of the magnetic levitation actuator is shown in Fig. 2. Since the control principles in the α and β directions are similar to those in the x and y directions, this paper focuses on the z, α, and x directions for analysis. In Fig. 2(a), the axial electromagnets generate a combined electromagnetic force that counteracts the platform's gravity, enabling motion along the Z-axis. In Fig. 2(b), differential moments generated by the left and right axial electromagnets induce rotation about the X-axis. Finally, in Fig. 2(c), the radial electromagnets exert a resultant force on the platform, resulting in translational motion along the X-axis.

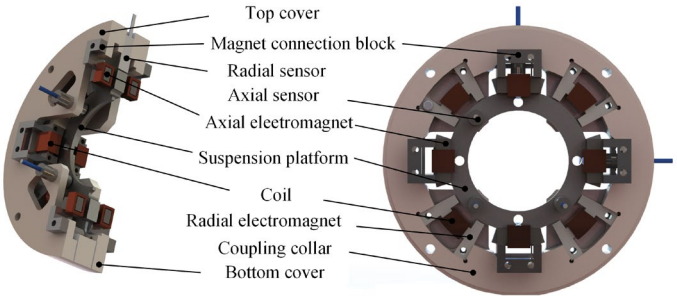

Fig. 1 5-DOF magnetic levitation actuator

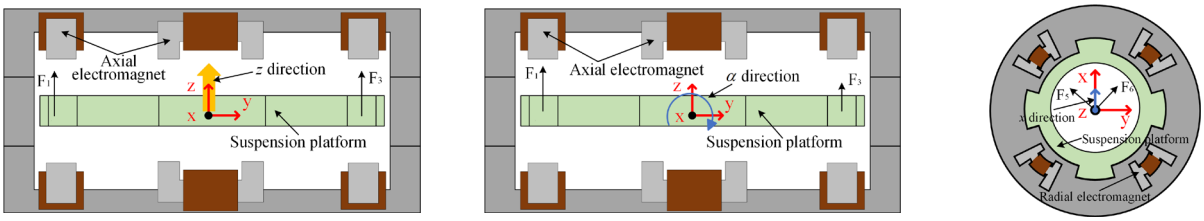

(a) (b) (c)

Fig. 2 Motion control principle of suspended platform (a) z direction. (b) α direction. (c) x direction.

2.2 System dynamics model

The forces and motions of the 5-DOF magnetic levitation actuator are illustrated in Fig. 3. By analyzing the forces and motions associated with each degree of freedom, the corresponding differential equations are derived. Applying a Taylor series expansion and neglecting higher-order terms, the linearized equation for stabilized levitation is obtained, as shown in equation (1):

$$\begin{cases} m\ddot{z} = K_i u_z + K_d z - c_z \dot{z} - mg + f_z \\ m\ddot{x} = \cos\theta(K_i u_x + K_d x) - c_x \dot{x} + f_x \\ m\ddot{y} = \cos\theta(K_i u_y + K_d y) - c_y \dot{y} + f_y \\ J_\alpha \ddot{\alpha} = K_i' u_\alpha + K_d' \alpha - c_\alpha \dot{\alpha} + T_\alpha \\ J_\beta \ddot{\beta} = K_i' u_\beta + K_d' \beta - c_\beta \dot{\beta} + T_\beta \end{cases} \tag{1}$$

In the above equation, F represents the magnetic force of the electromagnet, θ denotes the angle between the sensor and the X-axis, and L_2 is the distance from the center to the axial electromagnet. The variables z, α, and β refer to the displacements of the levitated platform along the Z-axis, the angle of rotation around the X-axis, and the angle of rotation around the Y-axis, respectively. Similarly, x and y denote the displacements along the X-axis and Y-axis, respectively. The mass of the levitated platform is denoted by m. The damping coefficients for the five degrees of freedom are represented by c_z, c_α, c_β, c_x, and c_y. The external perturbations for the five degrees of freedom are given by f_z, f_x, f_y, T_α, and T_β. Finally, J_α and J_β denote the moments of inertia around the X-axis and Y-axis, respectively.

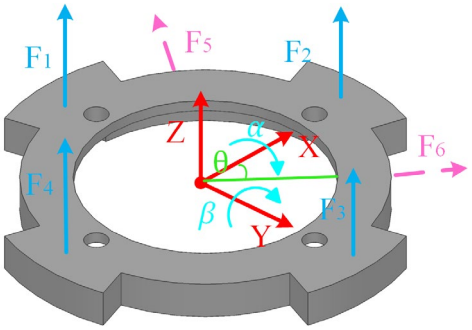

Fig. 3 Force analysis of suspended platform.

Table 1 Model parameter

Symbol	Quantity	Units
m	0.3	kg
J_α	9.7×10^{-4}	kg·m^2
J_β	9.7×10^{-4}	kg·m^2
K_i'	1.13	N/A
K_d'	1.7×10^{3}	N/m
K_i	1.13	N/A
K_d	1.7×10^{3}	N/m
c_z	0.3	kg/s
c_α	9.7×10^{-4}	kg·m^2/s
c_β	9.7×10^{-4}	kg·m^2/s
c_x	0.3	kg/s
c_y	0.3	kg/s
L_2	49.6	mm
θ	45	Degree

3. Backstepping controller design and simulation analysis

3.1 Backstepping controller design

For brevity, "backstepping control" is abbreviated as BC. Eq. (2) represents the linearized dynamics model. To facilitate understanding of the BC design process, the z BC is used as an example. First, the state-space equations are rewritten in strict feedback form as follows:

$$\begin{cases} \dot{z}_1 = z_2 \\ \dot{z}_2 = \dfrac{K_i u_z}{m} + \dfrac{K_d z_1}{m} - \dfrac{c_z z_2}{m} - g + \dfrac{f_z}{m} \\ y = z_1 \end{cases} \tag{2}$$

First, define the z-degree-of-freedom tracking error as

$$e_z = z_{1d} - z_1 \tag{3}$$

where z_{1d} is the desired displacement trajectory. The Lyapunov function is chosen

$$V_1 = \frac{1}{2} e_z^{\,2} \tag{4}$$

Calculate the derivative of (4) as

$$\dot{V}_1 = e_z \dot{e}_z = e_z \left(\dot{z}_{1d} - z_2 \right) \tag{5}$$

Considering z_2 as a virtual control quantity, the desired virtual control z_{2d} is

$$z_2 = \dot{z}_{1d} + k_1 e \tag{6}$$

where k_1 is a positive number and $k_1 e$ denotes the virtual control law in the first subsystem. Summing Eq. (6) into Eq. (5) yields:

$$\dot{V}_1 = -k_1 e_z^{\,2} \le 0 \tag{7}$$

According to Lyapunov's theorem, the system is asymptotically stable when $V_1 > 0$ and $\dot{V}_1 \le 0$, indicating that the suspended platform displacement can track the desired displacement.

The error between the virtual control z_2 and the desired virtual control z_{2d} can be obtained through Eq. (7) as

$$\delta_z = z_{2d} - z_2 \tag{8}$$

$$\dot{\delta} = \dot{z}_{2d} - \dot{z}_2 = \ddot{z}_{1d} + k_1 e_z - \frac{K_i u_z}{m} - \frac{K_d z_1}{m} + \frac{c_z z_2}{m} + g - \frac{f_z}{m} \tag{9}$$

Select Lyapunov function V_2

$$V_2 = \frac{1}{2} e_z^{\,2} + \frac{1}{2} \delta_z^{\,2} \tag{10}$$

Calculate the derivative of (10) as

$$\dot{V}_2 = e_z \dot{e}_z + \delta_z \dot{\delta}_z = -k_1 e_z^{\,2} + e_z \delta_z + \delta_z \left(\dot{\delta}_z \right) = -k_1 e_z^{\,2} + \delta_z \left(\dot{\delta}_z + e_z \right) \tag{11}$$

According to Lyapunov's theorem, in order to stabilize the system.

$$\dot{V}_2 = -k_1 e_z^{\,2} - k_2 \delta_z^{\,2} \le 0 \tag{12}$$

where $k_1 > 0, k_2 > 0$. The system is asymptotically stable when $V_2 > 0$, $\dot{V}_2 \le 0$.

Bringing Eq. (3) and Eq. (8) into Eq. (11), the control law u_z for the z degree of freedom is given by

$$u_z = \frac{m}{K_i} \left[e_z + \ddot{z}_{1d} + k_1 \dot{e}_z - \frac{K_d z_1}{m} + g + \frac{c_z z_2}{m} + k_2 \delta_z - \frac{f_z}{m} \right]$$

The above is the derivation of the backstepping control rate for the z, which is similar for the other degrees of freedom.

3.2 Simulation analysis

To evaluate the dynamic performance of the proposed backstepping control method, numerical simulations were conducted based on the established dynamic model of the five-degree-of-freedom magnetic levitation actuator. The simulation sampling period was set to 0.001 s, consistent with the actual system. To assess the controller's

performance, both backstepping control and PID control strategies were implemented in the magnetic levitation drive system. Their response speed and overshoot suppression capabilities under step input signals were compared using simulation software.

Owing to the structural symmetry of the actuator, three representative degrees of freedom—z, α, and x—were selected for simulation analysis. The initial position of the levitated platform was set to (0 mm, 0°, 0°), and the target equilibrium position was set to (0.1 mm, 0°, 0°). As shown in Fig. 4, step inputs were applied sequentially at 0.5 s, 2.5 s, and 4.5 s to the z, α, and x directions, respectively, and the corresponding system responses under both control strategies were compared. When a 0.1 mm step input was applied to the z direction at 0.5 s, the BC exhibited a maximum overshoot of 24% and stabilized within approximately 0.02 s, while the PID controller showed a significantly higher overshoot of 300% with a settling time of around 0.86 s. When a 0.1° step input was applied to the α direction at 2.5 s, the BC achieved an overshoot of 9% and stabilized within 0.25 s, whereas the PID controller exhibited an overshoot of 260% and a settling time of approximately 0.6 s. Finally, for a 0.1 mm step input applied to the x direction at 4.5 s, the BC achieved a minimal overshoot of 8% with a fast response time of 0.01 s, compared to 210% overshoot and 0.64 s settling time for the PID controller.

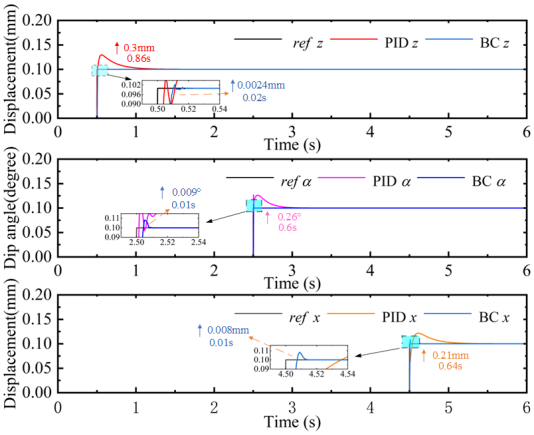

Fig. 4 Step response simulation for PID and BC.

The simulation results demonstrate that the designed BC significantly outperforms the conventional PID controller in multi-degree-of-freedom control, exhibiting smaller overshoot and faster response. Particularly in the strongly coupled, multi-input multi-output magnetic levitation system, BC more effectively suppresses nonlinear dynamic effects and ensures rapid and stable tracking of the desired trajectory.

4. Experimentation and analysis

4.1 Experimental system

To validate the simulation results, physical experiments were conducted using the five-degree-of-freedom magnetic levitation drive system developed in this study. The experimental setup implements the proposed BC strategy. As shown in Fig. 5, the experimental prototype comprises a five-degree-of-freedom magnetic levitation actuator, a dSPACE-based control system, a displacement sensing unit, and a power drive module. The controller sampling frequency is set to 1 kHz to meet the high-speed response requirements of the system.

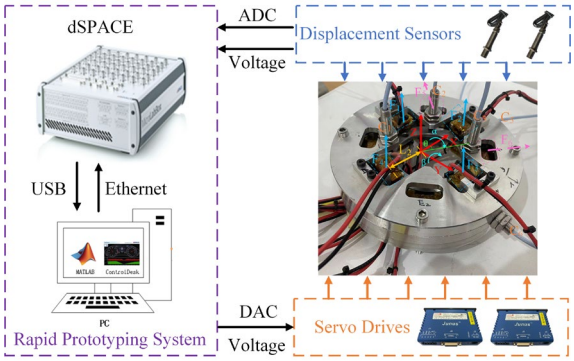

Fig. 5 5-DOF magnetic levitation actuator experiment system

4.2 Axial multi degree of freedom control

To further promote the engineering applications of magnetic levitation drives in laser processing equipment—such as shaped hole machining and complex trajectory cutting—it is essential to achieve coordinated multi-degree-of-freedom control of the platform.

Therefore, this paper conducts multi-degree-of-freedom control experiments on a five-degree-of-freedom magnetic levitation actuator prototype to verify the control strategy's response characteristics and effectiveness under coupled interference conditions. Initially, the controller stabilized the levitated platform at the equilibrium position (0.6 mm, 0°, 0°). At 0.5 s, a 0.001° step input was simultaneously applied to the α and β degrees of freedom, while the response of the z degree of freedom was recorded.

Figure 6 illustrates the multi-degree-of-freedom control response of the PID controller following the step input. The maximum overshoot reached 160% for the α degree of freedom with a response time of 0.52 s, and 320% for the β degree of freedom with a response time of 0.36 s. Due to coupling effects, the z degree of freedom was perturbed but returned to equilibrium within approximately 0.25 s, indicating sensitivity to dynamic disturbances. In contrast, Fig. 7 shows the axial multi-degree-of-freedom response under the BC strategy. The maximum overshoots of the α and β degrees of freedom were reduced to 120% and 115%, respectively, with response times significantly shortened to 0.05 s and 0.07 s. The z degree of freedom was nearly unaffected by attitude perturbations, demonstrating stronger anti-coupling capability. However, under BC, small high-frequency oscillations appeared in the response curves along with some steady state error. This is mainly attributed to the increased control gain required by the controller to maintain stability under external disturbances and noise, which leads to stronger control currents and induces control jitter.

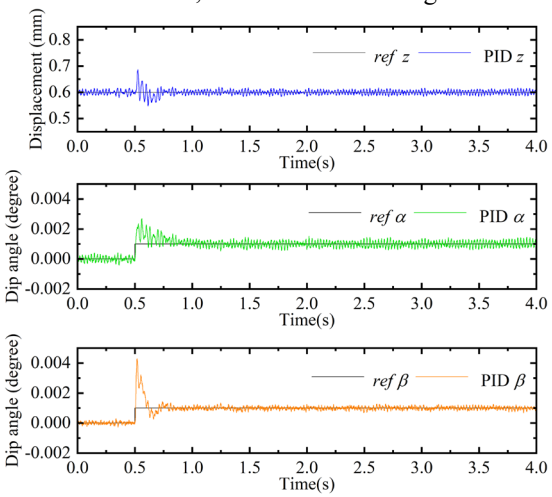

Fig. 6 PID axial multi degree of freedom experiment

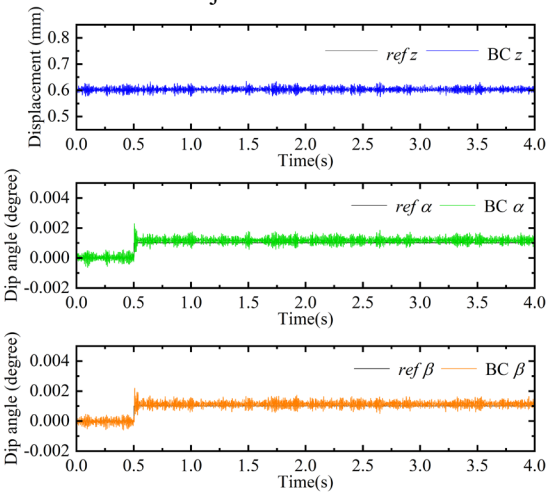

Fig. 7 BC axial multi degree of freedom experiment

Overall, the experimental results indicate that BC outperforms PID control in terms of response speed and anti-coupling performance but still requires further optimization for noise robustness and oscillation suppression.

4.3 Radial multi degree of freedom control

To further evaluate the dynamic performance of multi-degree-of-freedom control in the translational direction, a simultaneous step input of 0.1 mm was applied to both the x and y degrees of freedom while the platform was stabilized at the equilibrium position (0.6 mm, 0°, 0°, 0 mm, 0 mm).

Figures 8 and 9 illustrate the radial multi-degree-of-freedom control responses under PID and BC strategies, respectively. As shown in Fig. 8, the x degree of freedom exhibits a maximum overshoot of 270% with a response time of approximately 0.50 s, while the y degree of freedom shows an overshoot of 240% and a response time of about 0.55 s. The system response demonstrates significant hysteresis and is notably affected by coupling interference among the degrees of freedom. In contrast, Fig. 9 reveals a marked improvement in response speed under backstepping control. The x degree of freedom overshoots by 220% with a response time of 0.15 s, and the y degree of freedom overshoots by 230% with a response time of 0.29 s. Compared to PID control, the BC enables faster system response and better suppression of large oscillations. However, some steady-state error remains, possibly due to external disturbances, model inaccuracies, or insufficient tuning of control gains.

Overall, the BC demonstrates superior dynamic performance in multi-degree-of-freedom composite control along the translational directions, particularly in terms of response time and overshoot reduction. Nevertheless, further research is necessary to explore error convergence mechanisms and robust regulation strategies.

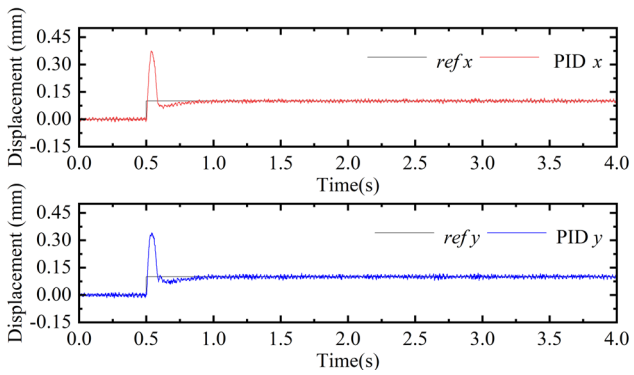

Fig. 8 PID radial multi degree of freedom experiment

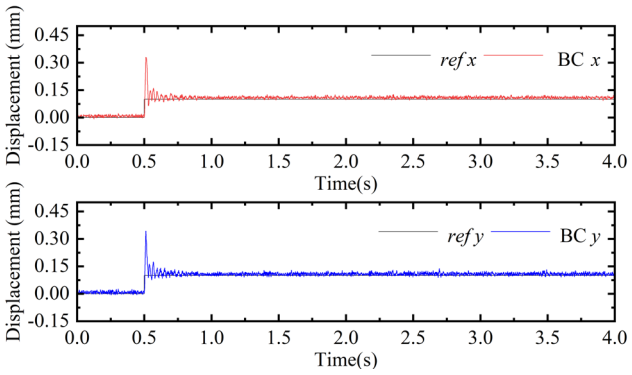

Fig. 9 BC radial multi degree of freedom experiment

5. Acknowledgments and conflicts of interest

Author contributions: Conceptualization, visualization: Feng LIU; Methodology, validation: Chuan ZHAO; Funding acquisition, project administration: Feng SUN; Data processing, formal analysis: Xu BAI; Supervision: Honglei SHA.

Acknowledgments to funding sources: National Key R&D Program of China (Grant No. 2024YFB3410002), the National Natural Science Foundation of China (Grants No. 52375258 and 52405284), and the Natural Science Foundation of Liaoning Province, China (Grants No. 2023-BSBA-263 and 2023-BS-127).

6. Conclusion

This paper proposes a BC strategy for magnetic levitation actuators in laser cutting applications, aimed at achieving high-response, high-precision multi-degree-of-freedom cooperative motion control. Through system modeling, controller design, simulation analysis, and experimental validation on a prototype platform, the results demonstrate that the proposed BC outperforms the PID controller in terms of overshoot, response time, and disturbance rejection capability. It also exhibits superior dynamic performance and control stability in multi-degree-of-freedom control scenarios. Considering that the current system still experiences some oscillations under coupled multi-degree-of-freedom perturbations, future work will focus on integrating a chattering suppression mechanism into the controller design and further optimizing control parameter tuning to enhance response smoothness and steady-state accuracy.

References

Seyedeh, F. N., Anooshiravan, F. and Hamid, D., An applicable review on recent laser beam cutting process characteristics modeling: geometrical, metallurgical, mechanical, and defect, The International Journal of Advanced Manufacturing Technology, Vol.130 (2024), pp.2159–2217.

Liu, G., Lu, Y., Xu, J., Cui, Z., Yang, H., Magnetic levitation actuation and motion control system with active levitation mode based on force imbalance, Applied Sciences, Vol.13, No.2 (2023), pp.740.

Zhao, C., Zhang, Q., Pei, W., Jin, J., Sun, F., Zhang, H., Zhou, R., Liu, D., Xu, F., Zhang, X., and Yang, L., Design and analysis of 5-DOF compact electromagnetic levitation actuator for lens control of laser cutting machine, Micromachines, Vol.15, No.5 (2024), pp.641.

Chen, Q., Tan, Y., Li. J., Mareels, I., Decentralized PID control design for magnetic levitation systems using extremum seeking, IEEE Access, Vol.6 (2017), pp.3059-3067.

Zhang, H., Zhang, Q., Shen, H., Lan, Y., Wen, J., and Zhao, C., Improve LADRC Strategy for variable air gap permanent magnetic levitation system, IEEE Access, Vol.15 (2025), pp.61641-61650.

Vimala, S. A., Sathiyavathi, S., Design of sliding mode controller for magnetic levitation system. Computers & Electrical Engineering, Vol.78 (2019), pp.184-203.

Zhang, Z., Li, X., Real-time adaptive control of a magnetic levitation system with a large range of load disturbance, Sensors, Vol.18, No.5 (2018), pp.1512.

Song, L., Dai, Y., Wang, L., Zhang, W., Ji, Y., Cao, Y., Motion control of capsule robot based on adaptive magnetic levitation using electromagnetic coil, IEEE Transactions on Automation Science and Engineering, Vol.20, No.4 (2022), pp.2720-2731.

Yao X, Chen Z B. Sliding mode control with deep learning method for rotor trajectory control of active magnetic bearing system, Transactions of the Institute of Measurement and Control, Vol.41, No.5 (2019), pp.1383-1394.

Zhu, P., Zhang, T., Zhou, D., Li, J., Jin, Y., Li, Q., Research on magnetic levitation control method under elastic track conditions based on backstepping method. Mathematics, Vol.12, No.13 (2024), pp.2134.

R.-J, W. and J.-D, L., Backstepping-based levitation control design for linear magnetic levitation rail system,

Mathematics, Vol.2, No.1 (2008), pp.72-86.
Hu, Q., Shao, X., Yang, H., Duan, C., Spacecraft attitude planning and control under multiple constraints: Review and prospects, Acta Aeronautica Astronautica Sinica, Vol.43, No.10 (2022), pp.527351-527351.
Xu B., Zhou, J., Xu, L., Vibration suppression for a slice rotor supported by active magnetic bearings based on fractional-order adaptive backstepping control, Mechanical Systems and Signal Processing, Vol.210 (2024), pp.111160.